J Low Temp Phys (2014) 175:464–470
DOI 10.1007/s10909-013-0962-y

Development of a Fiber-Optic Probe Hydrophone for a Cryogenic Liquid

K. Obara · H. Ohmura · C. Kato · H. Yano · O. Ishikawa · T. Hata

Received: 1 July 2013 / Accepted: 23 October 2013 / Published online: 7 November 2013

Abstract We report the progress of developing a fiber-optic probe hydrophone (FOPH) system applicable to the measurement of local density/pressure fluctuations in a cryogenic liquid. The measurement principle is based on a law of classical optics known as "Fresnel's reflection loss." We use this principle at the end-face of a single-mode optical fiber that is immersed in liquid helium. Since the refraction index of liquid ^{4}He is a function of density, and the refraction index of the core of the optical fiber is constant, the pressure can be obtained by measuring the reflectivity. We have succeeded in measuring the temperature dependence of the static density, and we go on to discuss the possibility of application to acoustic pressure measurements.

Keywords Cryogenic sensor · Hydrophone · Local pressure probe · Acoustics

1 Introduction

Cavitation is the formation and immediate implosion of cavities in a liquid, and is well studied in research fields such as oceanic engineering, chemical and biomedical engineering and ultrasonic-cleaning applications. Almost all research on cavitation to date has been conducted from an engineering approach; that is, investigations have mainly focused on cavitation applications in water. Water is a complex substance, and as a result, it is hard to understand the fundamental mechanism of cavitation with it, for example, water contains a lot of impure gas and solid particles, which act as nucleation sites [1]. Liquid ^{4}He provides a means of understanding the fundamental mechanism of cavitation; whether a classical fluid or a quantum fluid, it is a super clean material that has no impurities at all because almost all substances freeze

K. Obara (✉) · H. Ohmura · C. Kato · H. Yano · O. Ishikawa · T. Hata
Department of Physics, Osaka City University, Sugimoto, Sumiyoshi-ku, Osaka 558-8585, Japan
e-mail: obara@sci.osaka-cu.ac.jp

and collect on the surface of the container or settle down at the bottom. Careful prefiltration with cryogenic traps can remove these substances completely. Moreover, since superfluid helium can be used to observe macroscopic quantum phenomena quite easily, a huge number of experiments have been carried out on it over the last hundred years, meaning that the thermodynamic and hydrodynamic properties have been well established [2]. The first observation of cavitation in liquid ^{4}He was by Finch [3], followed by Akulichev [4]. The most important studies have been done by Maris and Balibar [5], who succeeded in reaching the spinodal limit of superfluid ^{4}He and establishing the physics involved in quantum nucleation of bubbles by using focused ultrasonic waves. Recently, Abe [6] succeeded in visualizing bubble formation. Here, the bubbles in pure liquid ^{4}He are vapor bubbles, whose dynamics can not be described simply using Minnaert's scheme [7] nor Rayleigh-Plesset's equation [8], but must be described by the vapor bubble theory that was introduced by Finch [9] and Hao [10]. One interesting consequence of the vapor bubble theory is that the lifetime of vapor bubbles in an acoustic pressure field is long and the natural frequency is low (within the audio frequency range). In contrast, gas bubbles in water have a very short lifetime and a higher (ultrasonic) natural frequency. Thus, if we apply strong acoustic waves continuously to liquid ^{4}He, then vapor bubbles are nucleated and may interact with the acoustic waves. Hence, the possibility of observing acoustic turbulence [11] is higher than in the case of gas bubbles in water. In previous experiments, we excited a large amplitude standing wave resonance in the audio frequency range to nucleate vapor bubbles and, at the same time, observed the random absorption and radiation of the acoustic waves caused by the acoustic turbulence. We also elucidated the random absorption and subharmonic excitation characteristics [12].

Using the findings of the previous research, we can measure the frequency with very high accuracy, but until now there has been no way to calibrate the absolute values of the acoustic pressure except for the experiment using the cryostat that has an optical window [13, 14]. It is very important to determine the cavitation threshold pressure [5, 15] and the pressure wave radiation from an oscillating bubble to understand acoustic turbulence. We need a hydrophone that can be used in a wider temperature and frequency range without using the optical window. The only candidate is a fiber-optic probe hydrophone (FOPH) [16], which has already been used for measuring the acoustic pressure in water [17], but has not yet been applied to a cryogenic liquid.

2 Experimental Principle and Apparatus

When light moves from a medium with refractive index n_1 into a second medium with refractive index n_2, both reflection and refraction of the light may occur. *Fresnel reflection and refraction* describe what fraction of the light is reflected and what fraction is transmitted at a flat, planar and uniform interface. The angles that the incident, reflected and refracted rays make to the normal of the interface are given as θ_i, θ_r and θ_t, respectively. The relationship between these angles is given by the law of reflection and Snell's law. The fraction of the incident power that is reflected from

the interface is given by the reflectivity R,

$$R = \left(\frac{n_1 \cos\theta_a - n_2 \cos\theta_b}{n_1 \cos\theta_a + n_2 \cos\theta_b} \right)^2, \tag{1}$$

where, the definitions of θ_a and θ_b depend on the angle of electric field polarization; $\theta_a = \theta_i$ and $\theta_b = \theta_t$ for the case when the field is parallel to the interface, and $\theta_a = \theta_t$ and $\theta_b = \theta_i$ for the case when it is perpendicular. However, in our experiment, the incident beam is designed to be perpendicular to the interface, so that the reflectivity formula is simplified with $\cos\theta_a = \cos\theta_b = 1$. We use a commercial optical fiber, in which the core has a refractive index of $n_f = 1.4583$ at room temperature. Its end-face is immersed in liquid helium so the reflection take places at the interface between the core of the fiber and the liquid helium. Since liquid helium is a dielectric medium, the refraction index is related to the density ρ by the Lorentz-Lorenz equation,

$$\frac{n(\rho)^2 - 1}{n(\rho)^2 + 2} = \frac{4\pi}{3} \frac{\alpha}{M} \rho, \tag{2}$$

where $\alpha = 0.123296$ cm^3/mol is the polarizability and $M = 4.0026$ g/mol is the molar mass of helium atoms [2]. Finally, the following relation is obtained,

$$R(\rho) = \left(\frac{n_f - n(\rho)}{n_f + n(\rho)} \right)^2. \tag{3}$$

This measurement principle is essentially the same as the density measurement done by Chavanne [13]. Our measuring method is simple at the point which we only treat the reflection at the fiber/helium interface, so that incident and reflected light are always confined to the optical fiber. Its benefit is represented by the following two points; first is that one does not need to prepare the cryostat with the optical window. Only one has to do is to introduce only one optical fiber into the existing cryostat. Second is that, the complicated light axis alignment is necessary only for the fiber-pigtailed laser diode, and the measurement will not be affected even if the cryostat and the optical system vibrated separately.

Now we show the experimental apparatus used to measure the reflectivity. Figure 1 shows the schematic diagram of our experimental setup. An infrared laser ($\lambda = 830$ nm) beam is injected into one port of the optical coupler, which is an optical two-way device that performs functions such as light branching. It is formed by joining two independent optical fibers, where the claddings of the fibers are fused over a small region. The devices work as a result of the energy transfer between the cores of the optical fibers, which is explained by the coupled-mode theory (CMT). We used an optical coupler with a branching ratio of $r = 0.5$. The incident power at the fiber-helium interface is $P_{in} = (1 - r)P_0$, and the power of the reflected light from the interface is $P_{ref} = R(1 - r)P_0$, which is split again at the optical coupler. One beam, whose power is $P_A = rP_{ref} = r(1 - r)RP_0$, is detected by the high sensitivity photo-diode (APD). The other tries to return to the source but is prevented by the isolator. At the same time, the incident power P_{in} can be determined directly by measuring the power P_B at the conventional photo detector (PD) as $P_B = rP_0$. Finally, the reflectivity can be obtained by

$$R = \frac{P_{\mathrm{ref}}}{P_{\mathrm{in}}} = \frac{1}{1-r}\frac{P_{\mathrm{A}}}{P_{\mathrm{B}}} = \chi \frac{V_{\mathrm{A}}}{V_{\mathrm{B}}}, \tag{4}$$

where V_{A} and V_{B} are the output voltages of the APD and PD, respectively. χ is an experimental constant that is calibrated at static pressure. In this experiment, we modulated the power of the laser at 70 kHz, and the output voltage of the PD and APD were read by a lock-in amplifier. And the contribution of the stray light S, that is in Eq. (4) in reference [16], is directly measured by putting the probe fiber directly into the index-matched liquid. In our system, S/R was less than 0.008, which is negligibly small. One of the biggest advantages of using a FOPH is that there is no frequency dependence of the optical system [16]. Hence, it is possible to calibrate the absolute value of the time-varying density/pressure using the well known density at hydrostatic pressure. The frequency dependence arises only from the photo-detector and the amplifier systems, whose characteristics are well known and controllable. Another advantage is that it is possible to measure the local density *in situ* of an area that is comparable in size to the cross section of the fiber core. In the case of measuring an acoustic pressure, the area will be the radius of the cladding of the bare fiber. A disadvantage, on the other hand, is that the sensitivity of the FOPH is not very high, and it is not favorable to increase the incident power because the temperature of the liquid will rise. Now we can show that the FOPH has a high density sensitivity. The density sensitivity of the system, $\Delta R/\Delta\rho$, can be roughly estimated as,

$$\frac{\Delta R}{\Delta \rho} = \frac{\partial R}{\partial n}\frac{\partial n}{\partial \rho} = -\frac{4n_{\mathrm{f}}(n_{\mathrm{f}}-n)}{(n_{\mathrm{f}}+n)^3}\frac{4\pi}{3}\frac{\alpha}{M}\frac{(n^2+2)^2}{6n} \approx -0.077\ \left[\mathrm{cm}^3/\mathrm{g}\right], \tag{5}$$

where, $n \sim 1.0$. According to Donnelly and Barenghi [2], the density of liquid ^{4}He at the saturated vapor pressure changes from $\rho_{5\ \mathrm{K}} = 0.106\ \mathrm{g/cm}^3$ to $\rho_{0\ \mathrm{K}} = 0.145\ \mathrm{g/cm}^3$. Thus, $\Delta R_{0\ \mathrm{K}\to 5\ \mathrm{K}} \approx -0.077 \times (0.145 - 0.106) = 0.3\ \%$. When the incident light power $\Delta P_{\mathrm{in}} = 1.5$ mW, then the reflected light power ΔP_{ref} will be 45 μW, which is detectable with an APD.

All optical systems are connected by commercial step-index single-mode silica fibers, whose characteristic dimensions are shown in Fig. 2(A). The end-face of the probe fiber is carefully cleaved so that laser can enter the interface perpendicularly, whose accuracy is less than 0.5 degree, as shown in Fig. 2(B). Careful reader will

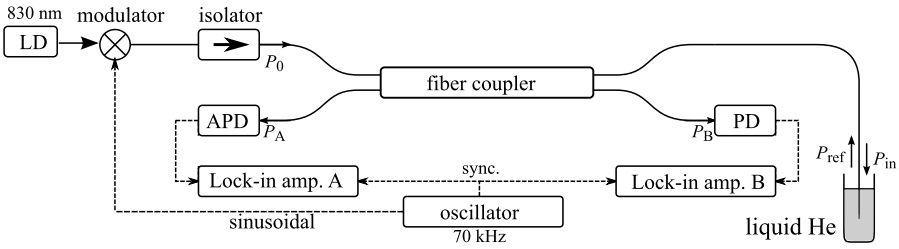

Fig. 1 Schematic diagram of experimental setup. *Solid lines* represent the single-mode optical fiber, and *dashed lines* represent the electrical signal wire. APD and PD are high-speed photo detectors. APD uses an avalanche photo-diode whose sensitivity is 3×10^5 [V/W]. PD uses a Si-photo-diode with a trans-impedance amplifier whose sensitivity is 4.7×10^3 [V/W]. P_x denotes the laser power at each point

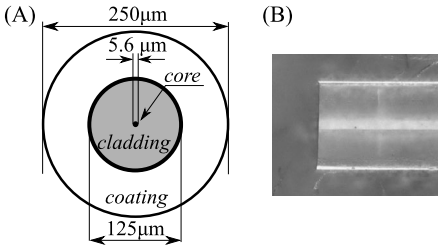

Fig. 2 (**A**) A schematic view of the probe fiber. The diameter of the core is considered to be the mode field diameter. All the numerical values quoted here are the manufacturer's guaranteed performance at 830 nm at room temperature. (**B**) Photograph of the cleaved end-face of probe fiber whose coating is removed

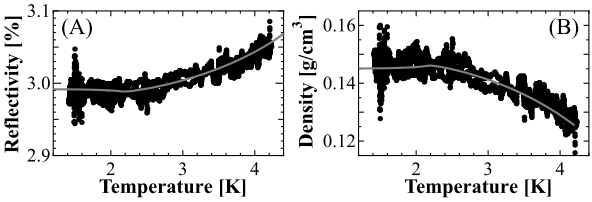

Fig. 3 (**A**) Temperature dependence of reflectivity R at end-face of the optical fiber immersed in liquid ^{4}He. (**B**) Calculated density. *Solid gray lines* show the theoretical values (*see text*)

notice that there is a layer of air between the PD and the optical fiber extending from the optical coupler, which causes another reflection. This is a nuisance; it would form a laser cavity in our optical fiber network. Since the mode of the laser in the cavity is very sensitive to change in its length, the mechanical vibration will cause a severe signal fluctuation. To prevent reflection, the end-face of the optical fiber to the PD is cut off at 8 degree. By doing so, reflected light from the fiber/air interface would be allowed to diffuse out of the fiber because it is impossible to satisfy the total reflection condition of the fiber. At the expense, the intensity is decreased by about 40 %. This loss is included in the χ in Eq. (4). The probe fiber is directly dipped into the liquid helium, and the liquid helium is cooled down by the classical bath-pumping method.

3 Results and Discussions

To evaluate the performance of our FOPH, we measured the density of liquid ^{4}He at saturated vapor pressure. Figure 3(A) shows the results for the reflectivity $R(\rho(T))$. Here, the fitting parameter $\chi = 0.0241$ was determined so as to fit the theoretical values, which are shown as a gray solid line in the figure for the entire temperature range. The theoretical values are calculated from Eq. (3) and [2]. Figure 3(B) shows the temperature dependence of the density calculated from Eq. (2) and $R(\rho(T))$, which agree with the well known values. It means that the temperature dependence of the refractive index of the probe fiber and the temperature-gradient dependence of the reflectivity are negligible, at least within our experimental accuracy. It can be understand as follows; Leviton [18] measured the refractive index of the silica-based optical fibers. By using their data, and assuming a step-like temperature variation along the fiber, we estimated that the additional reflectivity due to the temperature gradient is about 10^{-5} %, whereas our experimental accuracy is about 10^{-3} %. Moreover, we confirmed that the reflection does not take place at the interface other than the end-face of the probe fiber since there is no temperature independent component in reflectivity.

It is apparent that we have succeeded in measuring the static density of liquid ^{4}He with a FOPH. However, in the present condition, the accuracy of the density measurement is unsatisfactory at approximately 7 %. It is lower by more than two orders of magnitude compared with the previous studies using the optical cryostats. Since the fluctuation does not depend on whether the ^{4}He is a normal fluid, superfluid or even in its vapor phase, the reason for the fluctuation must be an instrumentation problem related to the temperature. The most likely problem is the fluctuation of the PD gain, which might be caused by the room-temperature dependence of the sensor itself or the feedback resister in the amplifier section. Particularly, we found a non-negligible long-term fluctuation in V_B. According to Eq. (4), the accuracy of the density ρ is strongly affected by the fluctuation of V_B; for example, a 1 % fluctuation in V_B gives rise to a 6 % fluctuation in ρ. The accuracy of the FOPH is strongly affected by the stability of the optical sensor, but it can be improved by introducing a temperature stabilizer to the sensor. Thus, our next mission is to reduce the fluctuation in the gain of the APD and PD. In addition to the cause described above, one may think about the stability of the output power of the LD, which is not sufficiently stable enough, in general. However, we always measured P_A, which is proportional to the power of the reflected light, and P_B, which is proportional to the power of the incident light, simultaneously. Since the power fluctuation of the LD gives rise to the in-phase fluctuation in P_A and P_B, and as seen from Eq. (4), the fluctuation of the power of the LD does not affect the reflectivity, which is a noteworthy advantage of this method.

There is also the possibility of observing the acoustic pressure, if the fluctuation is improved. First of all, we must determine the detailed the equation of state for liquid helium, $p_\mathrm{L} = p_\mathrm{L}(\rho, T)$. The pressure sensitivity can be written as,

$$\frac{\Delta R}{\Delta p_\mathrm{L}} = \frac{\Delta R}{\Delta \rho}\left(\frac{\partial p_\mathrm{L}}{\partial \rho}\right)^{-1}. \tag{6}$$

At this moment, we only know the equation for the case of $T \to 0$ that was formulated by Maris [19]. By using it as an estimation, the pressure sensitivity becomes $\Delta R/\Delta p_\mathrm{L} \approx -5.6 \times 10^{-3}$ [%/bar], which is too small to observe the acoustic pressure. So, we are now seeking another breakthrough technique that can improve the accuracy of our FOPH.

4 Conclusion

We measured the temperature dependent static density of liquid helium at saturated vapor pressure using a fiber-optic probe hydrophone with an optical coupler for the first time, the results of which agreed with the well known value. At this moment, the accuracy is not higher than the previous work done by Chavanne et al. using an optical window, but will be improved by introducing a temperature stabilizer to the optical sensor. After the improvement, our FOPH will enable us not only to measure the cavitation threshold of large amplitude sounds but also to get the time dependent spatial image of the pressure field by arraying the probe fibers. The advantage of this system is that it is possible to introduce the sensor directly to the conventional cryostat that has no optical window. We believe that the progress brought about by the FOPH offers a new viewpoint on low temperature physics.

Acknowledgements We thank K. Tojo of Chuo University and R. Nomura of Tokyo Institute of Technology for fruitful discussions. We acknowledge support from a Grant-in-Aid for Young Scientists (B) (Grant No. 22740201 and 24740206) from The Ministry of Education, Culture, Sports, Science and Technology (MEXT) of Japan.

References

1. A.A. Atchley, A. Prosperetti, J. Acoust. Soc. Am. **86**, 1065 (1989)
2. R.J. Donnelly, C.F. Barenghi, J. Phys. Chem. Ref. Data **27**, 1221 (1998)
3. R.D. Finch, R. Kagiwada, M. Barmatz, I. Rudnick, Phys. Rev. **134**, A1425 (1964)
4. V.A. Ackulichev, Ultrasonics **24**, 8 (1986)
5. S. Balibar, J. Low Temp. Phys. **129**, 363 (2002)
6. H. Abe, M. Morikawa, T. Ueda, R. Nomura, Y. Okuda, S.N. Burmistrov, J. Fluid Mech. **619**, 261 (2009)
7. M. Minnaert, Philos. Mag. A **16**, 235 (1933)
8. B.E. Noltingk, E.A. Neppiras, Proc. Phys. Soc. Lond. Ser. B **63**, 674 (1950)
9. R.D. Finch, E.A. Neppiras, J. Acoust. Soc. Am. **53**, 1402 (1973)
10. Y. Hao, A. Prosperetti, J. Acoust. Soc. Am. **11**, 2008 (1999)
11. W. Lauterborn, U. Paritz, J. Acoust. Soc. Am. **84**, 1975 (1988)
12. K. Obara, Y. Kimura, A. Fukui, C. Kato, Y. Nago, H. Yano, O. Ishikawa, T. Hata, J. Phys. Conf. Ser. **400**, 012057 (2012)
13. X. Chavanne, S. Balibar, F. Caupin, Phys. Rev. Lett. **86**, 5506 (2001)
14. F. Souris, J. Grucker, J. Dupont-Roc, Ph. Jacquier, J. Phys.: Conf. Ser. **400**, 012069 (2012)
15. D.W. Oxtoby, D. Kashchiev, J. Chem. Phys. **100**, 7665 (1994)
16. J. Staudenraus, W. Eisenmenger, Ultrasonics **31**, 267 (1993)
17. K. Davitt, A. Arvengas, F. Caupin, Europhys. Lett. **90**, 16002 (2010)
18. D.B. Leviton, B.J. Frey, T.J. Madison, Cryog. Opt. Syst. Instrum. **XII**, 669204 (2007)
19. H.J. Maris, J. Low Temp. Phys. **94**, 125 (1994)